Characterization of *Corypha umbraculifera* Petiole Fiber for Polymer Composite Reinforcement

B. G. N. P. Jayasooriya and S. A. S. C. Samarasinghe*

Department of Polymer Science, Faculty of Applied Sciences, University of Sri Jayewardenepura

Date Received: 30-09-2025 Date Accepted: 25-12-2025

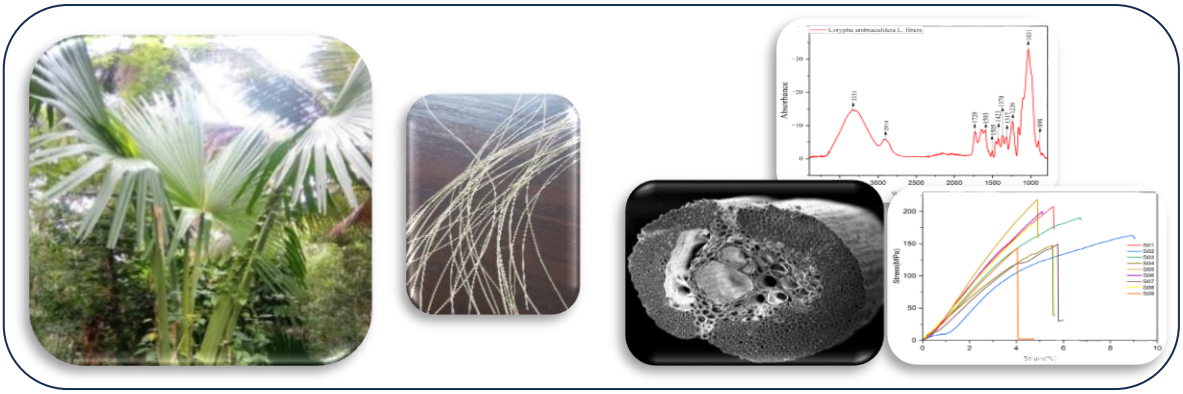

Abstract

Natural fiber composites are a sustainable alternative to traditional synthetic options. The study aims to investigate the potential of *Corypha umbraculifera* fibers as an unorthodox reinforcing filler for biodegradable polymer matrices. Chemical, thermal, density, mechanical, crystallographic, and morphological characterizations of the *Corypha umbraculifera* fibers were determined. The cellulose, hemicellulose, lignin, and moisture contents of the fibers were obtained as 66.37, 20.51, 6.25 and 9.80%, respectively. The peak at 3331 cm^{-1} in the FTIR spectrum indicate the presence prominent O–H stretching vibrations of the cellulose. The crystallinity index and the crystallite size of the fibers were obtained as 43.60% and 3.89 nm, respectively. The fiber has 178.02 ± 28.60 tensile strength, 39.14 ± 5.97 Young's modulus, and 2.73±0.37% maximum breaking elongation. Microfibril angle was obtained as 18.32 ± 1.28°, influencing fiber axial strength. Degradation temperature of the fibers was determined as 323.3°C, suggesting suitability for high-temperature applications. Porous fiber morphology leads to a density value of around 0.52 g/cm^3 indicating suitability for applications requiring lightweight composites. The green composite prepared by incorporating this *Corypha umbraculifera* fiber into poly lactic acid polymer matrix displayed a significant 17.5% increase for tensile strength at 5wt% fiber loading whereas 68.28% increase was observed for flexural strength at 2.5wt% fiber loading indicating the viability of synthesizing biodegradable composites with enhanced mechanical properties. Upon thorough examination of the characteristics in this study, it was established that fibers extracted from *Corypha umbraculifera* offer a promising and environmentally friendly choice as a reinforcement material for polymer-based composites.

Keywords: *Corypha umbraculifera, Fiber, Cellulose, Palm, Poly Lactic Acid*

*Correspondence: sulashisama@sjp.ac.lk

1. Introduction

Natural Fibers have gained significant importance in various industries such as textile, automotive, packaging, and construction due to their numerous benefits. They offer advantages such as renewability, sustainability, biodegradability, and low cost, and are less hazardous to health compared to synthetic fibers which are derived from petrochemical sources (Alhijazi et al., 2020; Kocak and Mistik, 2015). Traditional fibers including cotton, rice husk, jute, kenaf, sugarcane, coconut fiber, pineapple fiber, etc. have been a focus of research for numerous researchers all over the world (Bhunia et al., 2023) due to their desirable properties such as high specific strength and modulus, flexibility during processing, and substantial resistance to corrosion and fatigue (Gholampour and Ozbakkaloglu, 2020).

Although the major constituent of plant-based fibers is cellulose, researchers have shown that their properties can differ depending on the organism as well as the species. Hence, the characterization of the *Corypha umbraculifera* fiber (CUF) for polymer-based green composites is the goal of this research work. It is a tropical monocarpic palm that is known as Thalipot palm belonging to the Arecaceae family, grown in a moist climate and is native to semi-wild coastal plains of southwestern India, Sri Lanka, Malaysia, and Myanmar (Aaliya et al., 2022; Navaf et al., 2020). Fibers were extracted from the petiole which connects the leaves to the trunk. (Trimen, 1975).

Talipot palm is one of the classic examples of a monocarpic perennial plant that grows for many years, flowers once, and dies. (Dong et al., 2014). This agro-waste has inspired this research. To the best of our knowledge, there are no prior studies regarding the characterization of the fibers extracted from the *Corypha umbraculifera* and its potential as a reinforcing filler. The objective of this study is to investigate the structural, mechanical, thermal and morphological properties of the fibers and study their suitability as a reinforcing filler for polylactic acid-based composites.

2. Materials and methods

2.1 Fiber extraction method

A *Corypha umbraculifera* plant (Figure 1a) located in the North-western province, of Sri Lanka was harvested. Its petiole was separated from the leaf and the spines in its margin were removed. The petiole was then sectioned into parts of about 500 mm and washed in tap water to eliminate dirt and dust. The dew retting method, an alternative to traditional water retting that prevents water pollution and putrid odor, was used to extract fibers (Lee et al., 2020). The cut petioles were left for 4 weeks to facilitate fiber separation. A gentle tapping of the cut petiole with a hammer aided in loosening the fibers, which were subsequently separated manually. Finally, the CUF were washed with distilled water and dried in a 50 °C oven for 12 hours to eliminate residual moisture.

Figure 1. Extraction process of CUF (a) Tree, (b) Petiole, (c) Washing, (d) Drying, (e) Extracted fibers

*Correspondence: sulashisama@sjp.ac.lk

2.2 Characterization methods

2.2.1 Determination of chemical composition

Plant fibers mostly consist of cellulose, lignin, and hemicellulose. The content of fibers determines their characteristics (Kılınc et al., 2018). Cellulose and hemicellulose content determination was conducted using the methodology outlined by Mylsamy and Rajendran (2010), a technique which has also been adopted more recently by Dalmis, Köktaş, et al. 2020. The fiber sample was grounded into a powder and dried in a 105 ℃ oven before the chemical analysis. For cellulose content analysis, 1 g of powdered sample was treated with a 1.72% sodium chlorite solution. A few drops of concentrated sulfuric acid were added to this solution. After an hour of refluxing, the excess fluid was eliminated, and the remaining sample was treated using the concentrated ammonia solution. Subsequently, the sample was thoroughly washed with distilled water, and the resulting sediment was dried. The cellulose content was determined based on the remaining residue. For hemicellulose content analysis, 1 g of powdered sample was treated with 10% NaOH solution at ambient temperature for 1.5 hours, followed by curing with a 5% HCl solution while stirring. After removing excess fluid, the resulting sample was further treated in an oven for one hour at 90 ℃. The reduction in the initial weight corresponds to the hemicellulose content.

2.2.2 ATR-FTIR analysis

Attenuated total reflectance–Fourier transform infrared spectroscopy (ATR–FTIR) technique was used to identify the functional groups. The FTIR-ATR spectrum of *COF* was obtained by using a Nicolet S10 FT-IR spectrometer. Spectrum was recorded with a scan rate of 40 scans per minute in the range of 500–4000 cm^{-1} wavenumber with a resolution of 2 cm^{-1}. About 3 cm long samples were cut from several places along the fiber and tested to confirm the uniformity of the fiber.

2.2.3 Determination of Density

The density of the fibers was determined by a pycnometer liquid immersion test. Liquid psychometry, similar to the Archimedes method, directly measures the specimen's volume. and adheres to the ASTM 792 standard also. (Rude et al., 2000). Density was calculated using the following formula by using 1 g of specimen and water as the liquid. Density(ρ) measurements were replicated 3 times to obtain a more accurate value. Eq. (1) defines the density formula.

$$\rho_{fiber} = \frac{(W_3 - W_1)}{[(W_2 - W_1) - (W_4 - W_3)]}\, \rho_{water} \qquad (1)$$

The formula uses ρ_{fiber} for CUF density (g/cm³), ρ_{water} for water density (0.997 g/cm³ at 25°C), W_1 for the empty pycnometer mass, W_2 for the water-filled pycnometer mass, W_3 for the pycnometer with fibers, and W_4 for the pycnometer with both water and fibers.

2.2.4 Thermogravimetric (TGA) analysis

To determine the thermal stability of CUF*s*, thermogravimetric analysis was carried out by using TA SDT 650 – Thermal Gravimetric Analyzer. It was performed by heating approximately 10 mg of the sample from room temperature to 800 ℃ at a rate of 10 ℃/min. The oxidation effect was eliminated by using an N_2 atmosphere for the analysis.

*Correspondence: sulashisama@sjp.ac.lk

2.2.5 X-ray diffraction (XRD) analysis

To evaluate the crystallinity index and crystallite size of CUF*s* under investigation, X-ray diffraction analysis was executed employing the Rigaku Ultima IV X-ray diffractometer with Cu–Kα radiation (Wavelength (Kα1)=1.540 Å) as the primary radiation source and set to 30 mA and 40 kV power. Scanning was done in the 5° -80° range with an incremental scanning rate of 20° /min. Fibers were ground to obtain a fine powder in order to put into the specimen holder.
The crystallinity index (CI) was determined by using the empirical formula proposed by Segal et al. 1959. [Eq. (2)]

$$CI = \frac{I_{200} - I_{am}}{I_{200}} \times 100\% \quad (02)$$

I_{200} is the peak that represents the peak at the maximum intensity at 2θ angle between 22° and 23° that represents the (200) lattice.

This peak shows both crystalline and amorphous diffraction. I_{am}, which is the minimum intensity value between the highest two peaks analyzes the intensity for diffraction of the amorphous part at a specific angle of 2θ, which falls between 18 ° and 19 ° (Segal et al., 1959; Dalmis et al., 2020). The determination of crystallite size (L) was done using the application of Scherrer's formula [Eq. (3)], utilizing the width of the diffraction pattern within the X-ray-reflected crystalline region as a key parameter. The L_{200} is calculated from the diffraction pattern obtained from the 200 lattice planes of cellulose (Manimaran et al., 2019).

$$L = \frac{K\lambda}{\beta cos\theta} \quad (03)$$

where K is the Scherrer constant (0.9), λ is the wavelength of the X-ray beam used, θ is the Bragg angle and β is the full width at half maximum (FWHM) of the peak.

2.2.6 Single fiber tensile test

The tensile properties of CUFs were determined using a dual-column computerized electronic universal test machine (Model: ETM-5). Tests included a loading rate of 1 mm/min and a 50 mm gauge length and a sample size of twenty fibers was examined to ensure the repeatability. (Dalmis et al., 2020). A fiber was attached to a piece of paper which was then carefully gripped by the test machine. With the mounting tab unstrained, both sides of the tab were cut very carefully with a pair of scissors along the cut line at mid-gage as per ASTM D3379 (Manimaran et al., 2019). The microfibril angle is a crucial parameter that influences the strength of fibers. In the current study, the calculation of the microfibril angle was performed using the Eq. (04) (Rajeshkumar et al., 2021)

$$\ln\left(1 + \left(\frac{\Delta L}{L}\right)\right) = -ln(cos \propto) \quad (04)$$

Where ΔL, L and α represents the elongation at break(mm), gauge length (mm) and microfibril angle in degrees respectively.

2.2.7 SEM observation

The surface and cross-sectional morphology of CUFs were analyzed using a Carl Zeiss Evo 18 model scanning electron microscope (SEM). SEM images were captured at varying magnifications, with an accelerating voltage of 20 kV for surface morphology and 10 kV for cross-

*Correspondence: sulashisama@sjp.ac.lk

sectional morphology. Before scanning, the fiber's surface was coated with an Au-Pd alloy through a sputter coating.

2.3 Internal mixing of the PLA and CUFs

A Hitech, 30-150 Model internal mixer with a maximum volume of 50 g was used to get the homogeneous mixture of PLA and CUFs with different compositions by melt mixing. The screw rotation speed was set to 450 rpm, and the mixing time and mixing temperature were set to 170 ºC and 5 minutes, respectively.

Various compositions comprising 50 g of PLA pellets and treated fiber samples were introduced into the preheated mixing chamber of the internal mixer and mixed homogeneously. Treated CUFs were incorporated into the PLA polymer matrix in 1%, 2.5%, 5%, 10%, and 20% weight percentages to produce PLA-fiber composites (Figure 2). After 5 minutes, the PLA-fiber composite was removed from the mixing chamber and cooled.

Figure Error! No text of specified style in document.. PLA-fiber composites after melt mixing with fiber composites **(a)** 1wt. % **(b)** 2.5 wt.% **(c)** 5 wt. % **(d)** 10 wt.% **(e)** 20 wt.%

2.4 Compression molding (hydraulic press) of the PLA-fiber composite

The PLA-fiber composite was compression molded into 160 × 160 × 3 mm^3 mold using a hydraulic compression molding machine. About 50 g of composite sample removed from the internal mixer was placed between two mold sheets. This compression molded process was carried out at 170 ℃ with a pressure of 20 tons and cooled for 5-7 minutes using a water-cooling system. A similar process was used to produce composite sheets for all the compositions of the composite.

3. Results and Discussion

3.1 Chemical composition analysis

The chemical compositions of the CUF are basically cellulose, hemicellulose, lignin, ash, and moisture contents. Research on different natural fibers suggests that an increased cellulose content is directly associated with enhanced mechanical characteristics like tensile strength and Young's modulus when used as reinforcement in composites. In this context Sri Lankan CUF has the added advantage of having a high cellulose content compared to other palm fibers in its family. However, the presence of hemi-cellulose on fiber surfaces has been found to have a negative impact, resulting in contrasting effects on mechanical properties (ArunRamnath et al., 2023). This problem was addressed through mild alkaline treatments to the fibers. The chemical compositions of various natural fibers of the palm family are given in Table 1. The constituents are varied due to growth rate, age, microstructure, climate conditions, type of soil and type of extraction of natural fiber. (Venkatachalam et al., 2016).

*Correspondence: sulashisama@sjp.ac.lk

Table 1. Comparison table of chemical compositions of *Corypha umbraculifera* with some recently characterized fibers

Fiber name	Cellulose content (%)	Hemicellulose content (%)	Lignin content (%)	Reference
***Corypha umbraculifera*(Thalipot Plam petioles)**	66.37	20.51	6.25	In current study
***Phoenix dactylifera* (Date palm plant petioles)**	61.13	12.56	19.91	Rajeshkumar et al., 2021
***Elaeis guineensis* (oil palm petiole fiber)**	39.83	31.04	21.15	Nneka et.al., 2021
***Hyophorbe verschaffeltii* Spindle Palm petiole**	40.65	31.23	21.62	Nneka et.al., 2021
***Roystonea oleracea* Caribbean royal palm petiole**	61.67	14.52	9.15	Gurupranes et.al., 2022
***Arenga pinnata* (Sugar palm)**	36.66	29.35	33.99	Mulla et.al.,2025

3.2 Density results

Determined density of CUF was 0.52 ± 0.009 g/cm^3. As the density value is lower than 1, these CUFs are exceptionally suitable for designing lightweight applications rather than prevalent cellulose fibers like Bamboo (0.6-1.1 g/cm^3), flex (1.4 g/ cm^3) and hemp (1.4 g/cm^3) (Lu et al., 2011).

3.3 ATR-FTIR analysis of CUFs

The ATR-FTIR spectrum (Figure 3) of the fiber reveals distinctive peaks associated with various functional groups and cellulose, hemicellulose, and lignin as the main components. The prominent O–H stretching vibrations at 3331 cm^{-1} indicate the presence of hydroxyl groups characteristic of cellulose (Rajeshkumar et al., 2021). C–H stretching vibrations at 2914 cm^{-1} are indicative of CH and CH_2 in cellulose and hemicellulose (Oh et al., 2005). Peaks at 1728 cm^{-1} and 1505 cm^{-1} correspond to ester groups in hemicellulose or carboxylic acid in lignin and the C=C stretching of aromatic lignin, respectively (Dalmis, et al. 2020; Kılınç et al. 2018). The peak at 1593 cm^{-1} can be an indication of H–O–H bending vibrations originating from water, indicating the fiber's moisture content. (Kilic, et al. 2020). Symmetric bending of CH_2 in cellulose is evident at 1423 cm^{-1}, emphasizing the structural characteristics of cellulose (Porras et al., 2015).

The peaks at 1370 cm^{-1}, and 1317 cm^{-1} suggest C–O bending vibrations in aromatic rings of hemicellulose (Sreenivasan et al., 2011). Moreover, the peak at 1239 cm^{-1} is indicative of C–O stretching vibrations in the acetyl groups of lignin (Keskin et al., 2020). The peak at 1031 cm^{-1} indicates the C–O stretching (César et al., 2015) and the peak at 898 cm^{-1} signifies the β-glycosidic linkages between monosaccharides, a distinctive feature of cellulose (Dalmis, et al. 2020).

*Correspondence: sulashisama@sjp.ac.lk

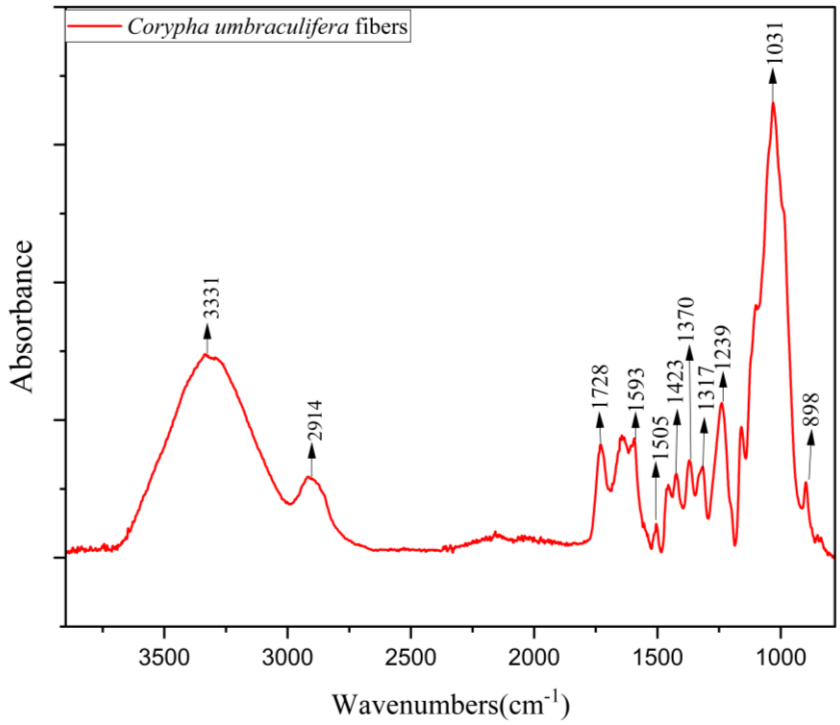

Figure 3. FTIR spectrum of the *Corypha umbraculifera* fibers

3.4 Thermogravimetric (TGA) analysis

Investigating the thermal stability of natural fibers plays a pivotal role in the advancement of natural fiber thermoplastic composites, as it sets an upper limit on the molding process temperature. To address this, the thermal decomposition behavior of *CUF* was investigated using TGA and the first derivative curve (DTGA) as shown in Figure 4. Three distinct stages of mass loss were observed. The initial weight loss 9.83% was observed at approximately 57℃ due to vaporization of the moisture content (Rajeshkumar et al., 2021).

As shown in Figure 4, the second decomposition marks the point at which the fibers begin to decompose which is known as the onset temperature of fibers (Dalmis, Kilic, et al., 2020). The last decomposition occurred due to lignin and alpha cellulose degradation (Porras et al., 2015). Maximum degradation temperature of the *Corypha umbraculifera* fibers is 323.3℃. According to Yao et al. 2008, mostly available and fibers like bagasse, bamboo, hemp, jute, kenaf, cotton, rice, and wood, the onset decomposition temperature range was about 215 ± 10 ℃ for almost all natural fibers and averaged at 219.5 ℃ for 10 types of fibers. However, CUFs have an onset temperature of approximately 263.6 ℃ (Figure 4), which is considerably higher than those. On the other hand, due to the higher onset temperature, fibers do not tend to degrade during the composite preparation conditions (170 ºC) (Nurazzi et al., 2021)

*Correspondence: sulashisama@sjp.ac.lk

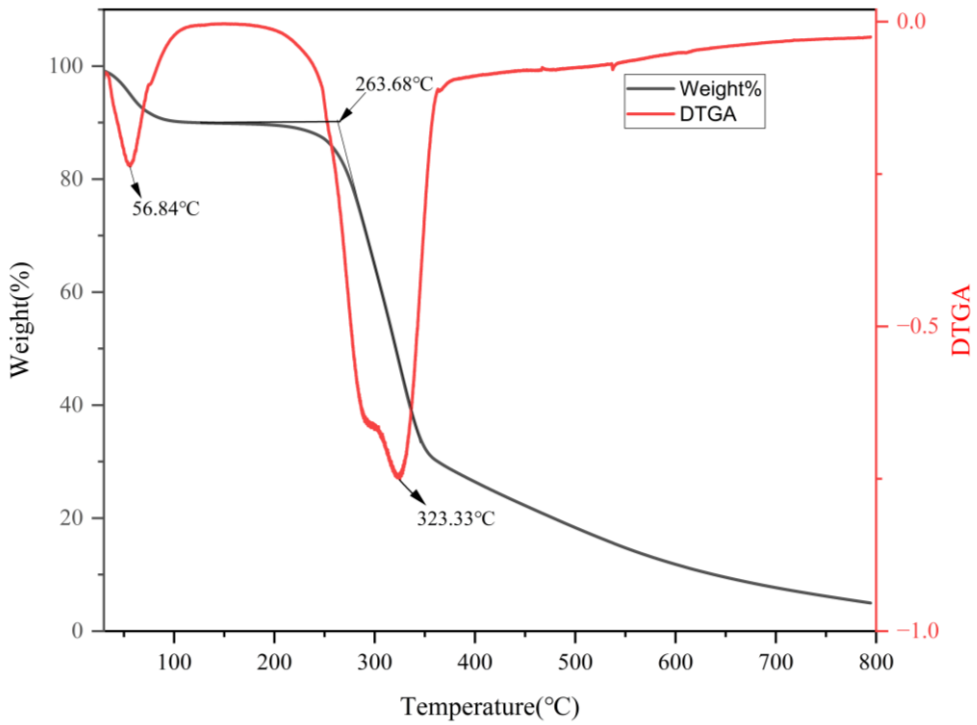

Figure 4. TGA/DTG curves of the *Corypha umbraculifera* fibers

3.5 XRD analysis

The X-ray diffraction pattern shown in Figure 5 reveals distinctive features associated with Cellulose I. A significant crystalline peak at 2θ = 22.14° corresponds to the (200) lattice plane, while an additional notable diffraction peak at approximately 2θ = 15.82° arises from the overlapping (110) and ($\bar{1}$10) lattice planes (Dalmis et al., 2020).

Additionally, a minor peak at around 2θ = 34.5° is indicative of the (004) plane (Keskin et al., 2020; Ling et al., 2019). The minimum intensity value between the main two peaks which is at 2θ =17.97° is an indication of amorphous region of the fibers. Such an amorphous region in the fiber comprises the presence of non-cellulosic constituents such as hemicellulose (ArunRamnath et al., 2023). The calculated crystallinity index is 43.65% indicating more amorphous regions compared to crystalline regions.

*Correspondence: sulashisama@sjp.ac.lk

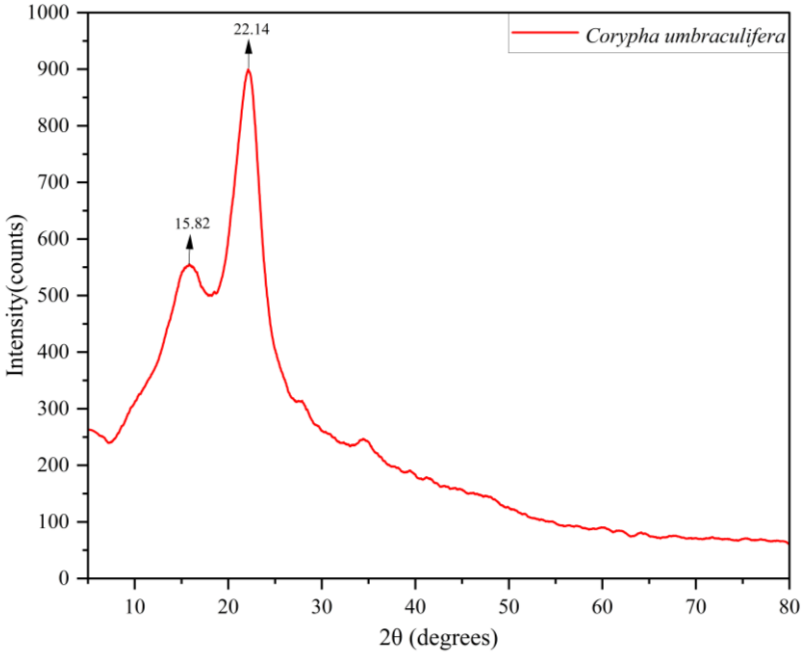

Figure 5. XRD graph of *Corypha umbraculifera* fibers

The calculated crystallite size of 3.89 nm is a key factor affecting water absorption. Fibers with smaller crystallite sizes tend to absorb more water (Gedik et al., 2021) and the crystallite size for some natural fibers are cotton fibers (5.5 nm), corn stalk fibers (3.8 nm) and flax fibers (2.8 nm) (Indran and Raj, 2015).

Table 2 Comparison of crystallinity index and crystallite size of cellulose-based fibers

Fiber	Crystallinity index(%)	Crystallite size(nm)	Reference
***Corypha umbraculifera* (Thalipot Palm)**	43.65	3.9	In current study
Chrysanthemum morifolium	65.18	4.1	(Dalmis et al., 2020)
Funacel	54	4.5	(Dalmis et al., 2020)
***Coccinia grandis*.L**	52.17	13.38	(Senthamaraikannan and Kathiresan, 2018)
Ficus religiosa	42.92	5.18	(Marcel et al,. 2020)
Flax	70	5.4	(Balaji and Nagarajan, 2017)
Ferula	48	1.6	(Balaji and Nagarajan, 2017)
Napier Grass Fiber Strands	62.43	2.83	(Balaji and Nagarajan, 2017)

3.6 Morphological characterizations

Scanning electron microscopy (SEM) was employed to investigate the surface morphology of CUFs at different magnifications, and the longitudinal and cross-sectional SEM images are depicted in Figures 6 and 7. For enhanced precision, SEM was used to determine the fiber diameter, resulting in an average diameter of 822.02 µm (±8.18).

*Correspondence: sulashisama@sjp.ac.lk

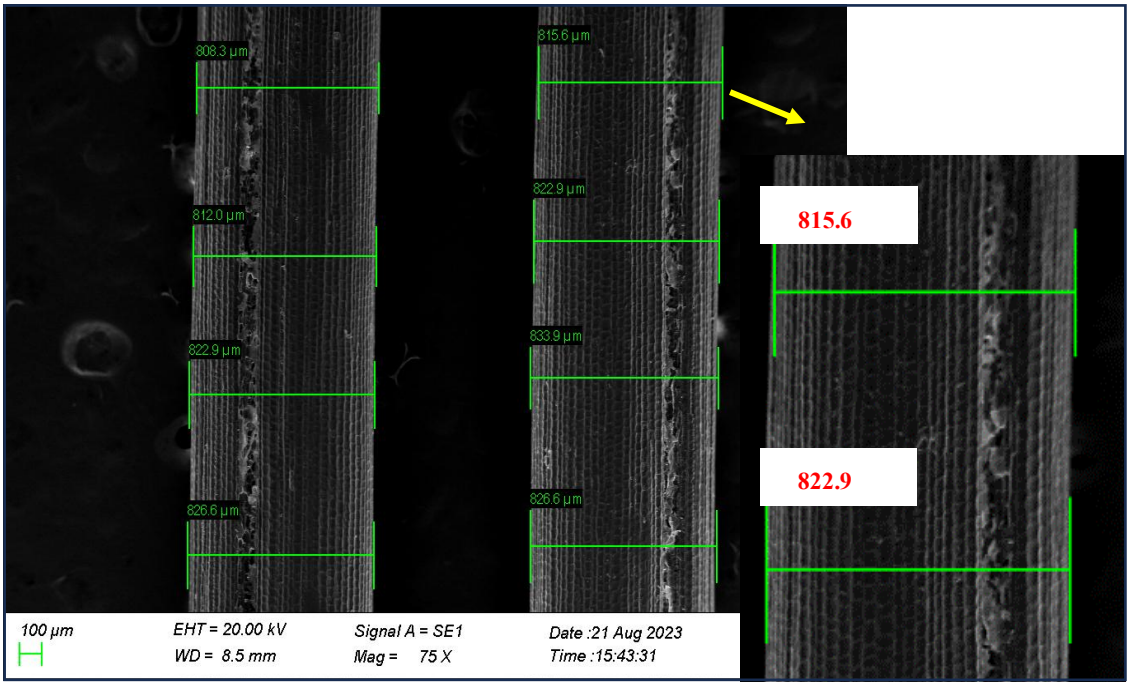

Figure 6. Diameter determination using SEM images

The surface morphology of a fiber is a very important factor in determining the ability of the fiber to act as a good reinforcement and to resist fiber pull out. The surface roughness contributes to increased contact surface area to ensure better adherence of the fiber with the matrix in composite manufacturing (Indran and Raj, 2015). Porous like patterns shown in the longitudinal images of SEM clearly show the surface roughness of the fiber and these irregularities endorse a big advantage with increased surface area. CUF exhibits a fiber bundle structure consisting of several elementary fibers like fibrils bonded together with pectin and non-cellulosic components and section geometry is an important parameter for composite applications (Keskin et al., 2020).

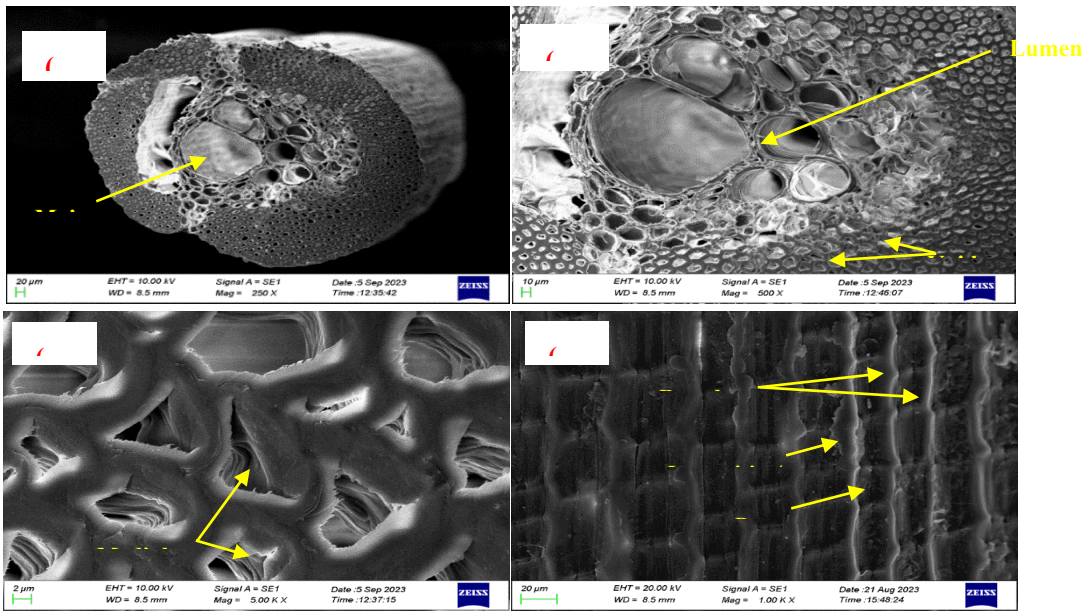

Figure 7. (a-c) Cross-sectional **(d)** Longitudinal SEM images of the *Corypha umbraculifera* fibers

*Correspondence: sulashisama@sjp.ac.lk

3.7 Single fiber tensile properties

The mechanical properties of fiber-reinforced composites depend on factors such as matrix composition, mechanical properties of the matrix, fiber orientation angle, fiber-matrix shear strength, adhesion, and reinforcement fiber properties. Controlling these parameters is crucial for tailoring the composite's strength (Huang and Netravali, 2009). Table 3 outlines the mechanical properties of CUFs, offering a comparative analysis with various natural fibers. The fibers display a brittle behavior, evidenced by a sudden decline in load upon fiber failure, as depicted in the stress-strain plot illustrated in Figure 8.

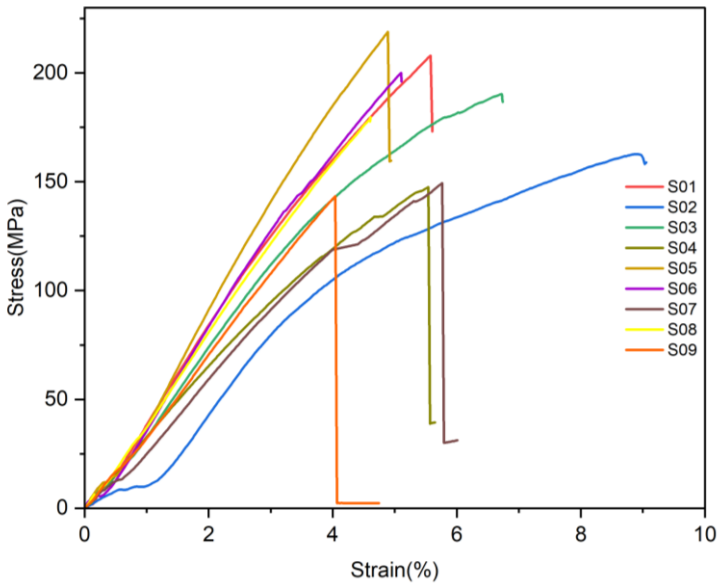

Figure 8. Stress–strain curves plot of *Corypha umbraculifera* fibers

Table 3. Comparison of diameter and Mechanical properties some recently characterized lignocellulosic fibers

Fiber	Diameter (µm)	Tensile strength (MPa)	Youngs Modulus (GPa)	Elongation at the break (%)	Reference
***Corypha umbraculifera*(Thalipot Palm)**	826.6 ± 8.18	178.02 ± 28.60	39.14 ± 5.97	2.74 ± 0.37	In current study
***Corchorus* (Jute)**	40–350	473	19.5	1.17 ± 0.2	(Vijay et al., 2019)
Oil palm	150–500	80–248	0.5–3.2	3.2 17–25	(Manimaran et al., 2018)
Coconut tree leaf sheath	140–990	46.4	2.3	2.84	(Moshi et al., 2020)
Pithecellobium dulce	144.3 ± 46.63	654.28 ± 36	6.81 ± 1.7	10.52 ± 1.4	(Manimaran et al., 2018)
Ficus Religiosa	25.62	433.32 ± 44	5.42 ± 2.6	8.74 ± 1.8	(Moshi et al., 2020)
Tridax procumbens	233.1 ± 9.9	25.75	0.94 ± 0.09	2.77 ± 0.27	(Vijay et al., 2019)

*Correspondence: sulashisama@sjp.ac.lk

The standard deviation in the mechanical properties of these fibers is notably large, a typical characteristic in natural fibers. This variance is likely influenced by factors such as the plant's age and origin, along with the presence of defects on the fiber surface, climatic conditions under which the plant grew, the circular transverse segment of the fibers, deviations in the fiber cell amounts from one bundle (Kilinc et al., 2018; Rajeshkumar et al., 2021).

The microfibril angle is a critical indicator of microfibrillar orientation, particularly impacting the axial strength properties of a fiber. Fiber stiffness and strength are highly sensitive to changes in the microfibril angle. Essential for high fiber strength are higher cellulosic content and a lower microfibril angle, as highlighted by Djafari Petroudy 2017. The calculated microfibril angle for CUFs is 18.32 ± 1.28°, closely aligning with those of other cellulosic fibers like Sisal (10-25°), confirming the suitability of CUFs for composite reinforcement. Reported microfibril angles for oil palm, abaca, softwood fiber, and banana fibers are 46°, 22.5°, 3-45°, and 11°, respectively (Djafari Petroudy, 2017).

3.8 SEM analysis of the PLA/CUF composite

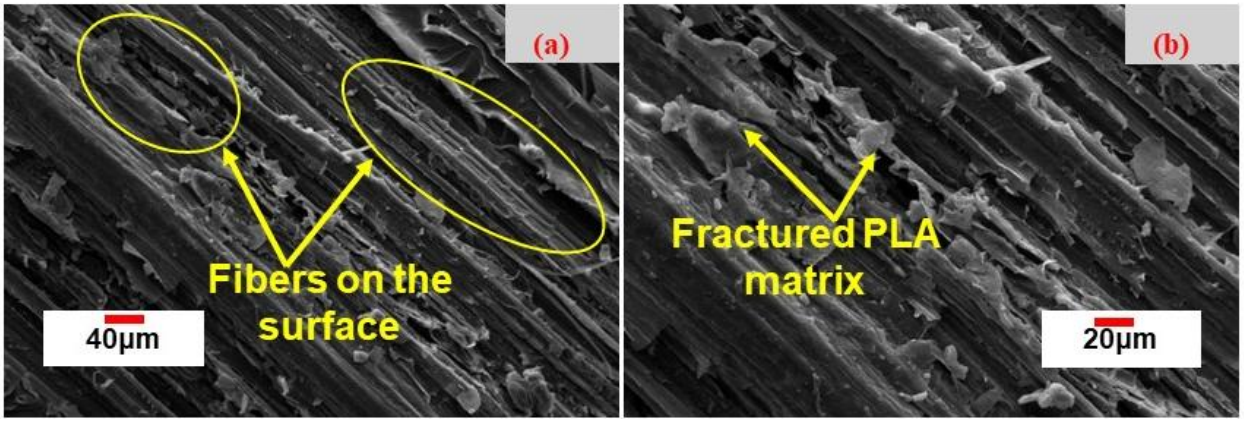

Figure 9. SEM images of the fractured surface of the tensile specimen

This SEM analysis suggests a good fiber-matrix interactions composite system where the fibers effectively contribute to strength. This observation is further proven by the obtained tensile results of the PLA/fiber composites, which is an increment of the tensile strength of the PLA/fiber composite compared to the pure PLA. The absence of fiber pull-out further shows good adhesion. During tensile testing, if the fiber-matrix bond is weak, the fibers tend to detach from the PLA matrix before breaking themselves. In this case, the absence of pull-out suggests a strong bond that allowed the fibers to share the load effectively with the PLA matrix.

3.9 Tensile strength of PLA/fibre composite

Table 4 depicts the tensile strength values for the neat PLA sample and the CUF incorporated PLA composites. Accordingly, the maximum amount that the fibers can be incorporated in to the polymer matrix is 5 %. Beyond this threshold value, tensile value starts to decrease. As such, maximum fiber-polymer interactions and load bearing situation can be achieved at the 5 wt% fiber compositions. Interestingly, this value is comparable to the tensile strengths reported by Gunti et.al for PLA-Sisal fiber composite (~66 MPa) and PLA-Elephant grass composite (~67 MPa) at 20 wt% fiber loadings (Gunti et.al., 2016).

*Correspondence: sulashisama@sjp.ac.lk

Table 4. Tensile strength of PLA and PLA-fiber composites

Sample No	Sample Name	Tensile Strength (MPa)
01	PLA	58.61 ± 0.08
02	PLA/1% fiber	62.72 ± 0.37
03	PLA/2.5% fiber	64.78 ± 1.93
04	PLA/5% fiber	68.96 ± 1.86
05	PLA/10% fiber	50.07 ± 2.22
06	PLA/20% fiber	37.39 ± 5.65

3.10 Flexural strength of PLA/fibre composite

According to the results presented in Table 5 flexural strength of neat PLA can be enhanced by incorporating CUF as reinforcements up to a threshold value of 10 wt% fiber. Flexural strength (3-point bending) measures the resistance of deformation under applied load. This shows the maximum stress experienced by the material within it at the moment of fracture. Incorporating fibers into a material can increase its flexural strength. The fibers act as reinforcement and absorb some of the stress applied, preventing the material from breaking as easily when bent. Based on the obtained results, the composite with 1%, 2.5%, 5%, and 10% fiber content (samples 2, 3, 4, and 5) exhibits a significant increase in flexural strength compared to pure PLA. CUFs emerge as a promising reinforcing agent for PLA. At high fiber concentrations (20% in sample 6), the fibers can be clumped together instead of uniform distribution. Poor adhesion between the CUFs and the PLA matrix can lead to reduced stress transfer, lowering the flexural strength.

Table 5. Flexural strength values of the PLA and PLA-fiber composites

Sample No	Sample Name	Flexural Strength (MPa)
01	PLA	41.08 ± 2.91
02	PLA/1% fiber	65.38 ± 1.36
03	PLA/2.5% fiber	69.13 ± 1.33
04	PLA/5% fiber	63.58 ± 1.35
05	PLA/10% fiber	62.40 ± 2.61
06	PLA/20% fiber	22.74 ± 2.18

3.11 Water contact angle of PLA/fibre composite

PLA due to the presence of ester groups inherently display a contact angle lower than 90° indicating hydrophilic properties. Interestingly, incorporation of CUF have further enhanced the hydrophilicity of the composites which was evident by the water contact angles (Table 6). On the other hand, enhanced hydrophilicity improves the biodegradability of the composite by facilitating hydrolysis as well as easy access to microbials.

Table 6: Water-contact angle measurements of the PLA and PLA-fiber composites

Sample No	Sample Name	Water-contact Angle (degrees)
01	PLA	66.167 ± 1.018
02	PLA/1% fiber	60.542 ± 0.504
03	PLA/2.5% fiber	59.024 ± 0.653

*Correspondence: sulashisama@sjp.ac.lk

04	PLA/5% fiber	57.643 ± 0.528
05	PLA/10% fiber	54.969 ± 0.734
06	PLA/20% fiber	47.676 ± 0.555

4. Conclusions

This study investigated the suitability of CUFs as a potential reinforcement material for green composites. The analysis revealed that the maximum degradation temperature as 323.3 ℃, indicating that these fibers could be used for industrial applications. The cellulose content was determined to be 66.37%, aligning with thermal analysis results. The hemicellulose, lignin, and moisture contents of *Corypha umbraculifera* fibers were 20.51, 6.25 and 9.8% respectively. The fibers exhibited a density of 0.52 ± 0.009 g/cm^3, and a tensile strength of 178.02 ± 28.60 MPa. High CI value of the fibers (43.6%) contributes to the improved mechanical properties and indicates that these fibers are suitable for formulating bio composites. The calculated microfibril angle was 18.32 ± 1.28°, impacting axial strength of the fibers. SEM images indicated a structure where elementary fibers were bonded together, and the hollow fiber morphology suggested potential benefits in insulation and absorption for lightweight composites. With its relatively high tensile strength, low density, and economic advantages in waste management, CUF emerges as a suitable candidate for green composites reinforcement. As such, the synthesized green composite, *Corypha umbraculifera* fiber-reinforced PLA matrix exhibit around 17 % and 50 % enhancement in tensile strength and flexural strength consecutively compared to neat PLA sample. As synthesize PLA-CUF composite would be an ideal candidate for light weight, high tensile strength applications with emphasize on biodegradability.

References

Aaliya, B. Sunooj, K. V., Krina, P. 2022. Determining the Effect of Plant Extracts on the Development and Characterization of Biodegradable Composite Films from Corypha Umbraculifera L. Stem Starch. Biology and Life Sciences Forum.20(1),13. https://doi.org/10.3390/iecbm2022-13393.

Alhijazi, Mohamad, Qasim Zeeshan, Babak Safaei, Mohammed Asmael, and Zhaoye Qin. 2020. Recent Developments in Palm Fibers Composites: A Review. Journal of Polymers and the Environment. 28(12),3029–54. doi: 10.1007/s10924-020-01842-4.

ArunRamnath, R., Murugan, S., Sanjay, M. R., Vinod, A., Indran, S., Elnaggar, A. Y., Fallatah, A. M., Siengchin, S.2023. Characterization of Novel Natural Cellulosic Fibers from Abutilon Indicum for Potential Reinforcement in Polymer Composites. Polymer Composites. 44 (1), 340–355. https://doi.org/10.1002/pc.27100.

Balaji, A. N., and K. J. Nagarajan. 2017. Characterization of Alkali Treated and Untreated New Cellulosic Fiber from Saharan Aloe Vera Cactus Leaves. Carbohydrate Polymers 174,200–208. doi: 10.1016/j.carbpol.2017.06.065.

Bhunia, A. K., Mondal, D., Parui, S. M., & Mondal, A. K. 2023. Characterization of a new natural novel lignocellulose fiber resource from the stem of Cyperus platystylis R.Br. Scientific Reports.13(9699). https://doi.org/10.1038/s41598-023-35888-w.

César, N. R., Pereira-da-Silva, M. A., Botaro, V. R., de Menezes, A. J.2015. Cellulose Nanocrystals from Natural Fiber of the Macrophyte Typha Domingensis: Extraction and Characterization. Cellulose. 22 (1), 449–460. https://doi.org/10.1007/s10570-014-0533-7.

Dalmis, R., Gonca B., Yasemin S., Serhan K., and Keskin, O. Y. 2020. Characterization of a Novel Natural Cellulosic Fiber Extracted from the Stem of Chrysanthemum Morifolium. Cellulose.

*Correspondence: sulashisama@sjp.ac.lk

27(15),8621–34. doi: 10.1007/s10570-020-03385-2.

Ganapathy, T., R. Sathiskumar, P. Senthamaraikannan, S. S. Saravanakumar, and Anish Khan. 2019. Characterization of Raw and Alkali Treated New Natural Cellulosic Fibres Extracted from the Aerial Roots of Banyan Tree. International Journal of Biological Macromolecules. 138,573–81. doi: 10.1016/j.ijbiomac.2019.07.136.

Gedik, G. 2021.Extraction of New Natural Cellulosic Fiber from Trachelospermum Jasminoides (Star Jasmine) and Its Characterization for Textile and Composite Uses. Cellulose**.** *1*. https://doi.org/10.1007/s10570-021-03952-1.

Gunti,R., Prasad, A.V. R. and Gupta, A.V.S.S.K.S.2016. Mechanical and Degradation Properties of Natural Fiber Reinforced PLA Composites: Jute, Sisal, and Elephant Grass.Polymer Composites.39(4), 1125-1136. doi.org/10.1002/pc.24041.

Huang, X., Netravali, A. 2009. Biodegradable Green Composites Made Using Bamboo Micro/Nano-Fibrils and Chemically Modified Soy Protein Resin. Composities Science and Technology.69 (7–8), 1009–1015. https://doi.org/10.1016/j.compscitech.2009.01.014.

Indran, S., Raj, R. E. 2015. Characterization of New Natural Cellulosic Fiber from Cissus Quadrangularis Stem. Carbohydrate Polymers. 117, 392–399. https://doi.org/10.1016/j.carbpol.2014.09.072.

Keskin, O. Y., Dalmis, R., Balci, G., Yasemin, K.2020. Extraction and Characterization of Cellulosic Fiber from Centaurea Solstitialis for Composites. Cellulose. 8. https://doi.org/10.1007/s10570-020-03498-8.

KılınÇ, A. Ç., Köktaş, S., Atagür, M.; Seydibeyoglu, M. Ö. 2018. Effect of Extraction Methods on the Properties of Althea Officinalis L. Fibers. Journal of Natural Fibers.15 (3), 325–336. https://doi.org/10.1080/15440478.2017.1325813.

Ling, Z., Edwards, J. V., Guo, Z., Prevost, N. T., Nam, S., Wu, Q., French, A. D., Xu, F.2019. Structural Variations of Cotton Cellulose Nanocrystals from Deep Eutectic Solvent Treatment: Micro and Nano Scale. Cellulose. 26 (2), 861–876. https://doi.org/10.1007/s10570-018-2092-9.

Manimaran, P., Sanjay M. R., Senthamaraikannan P., Mohammad Jawaid, and Raji George. 2018. Synthesis and Characterization of Cellulosic Fiber from Red Banana Peduncle as Reinforcement for Potential Applications. Journal of Natural Fibers.1–13. doi: 10.1080/15440478.2018.1434851.

Manimaran, P., Sanjay M. R., Senthamaraikannan P., Yogesha B., Claudia Barile, and Suchart Siengchin. 2018. A New Study on Characterization of Pithecellobium Dulce Fiber as Composite Reinforcement for Light- Weight Applications Composite Reinforcement for Light-Weight Applications. Journal of Natural Fibers. 1–12. doi: 10.1080/15440478.2018.1492491.

Manimaran, P., P. Senthamaraikannan, M. R. Sanjay, and M. K. Marichelvam. 2018. Study on Characterization of Furcraea Foetida New Natural Fiber as Composite Reinforcement for Lightweight Applications. Carbohydrate Polymers. 181,650–58. doi: 10.1016/j.carbpol.2017.11.099.

Manimaran, P., Sanjay, M. R., Senthamaraikannan, P., Jawaid, M., Saravanakumar, S. S., George, R. 2019. Synthesis and Characterization of Cellulosic Fiber from Red Banana Peduncle as Reinforcement for Potential Applications. Journal of Natural Fibers. 16 (5), 768–780. https://doi.org/10.1080/15440478.2018.1434851.

Moshi, A. A. M., Ravindran D., Bharathi S. R. S., S., Indran S., Saravanakumar S., and Liu Y. 2020. Characterization of a New Cellulosic Natural Fiber Extracted from the Root of Ficus Religiosa Tree. International Journal of Biological Macromolecules. 142,212–21. doi: 10.1016/j.ijbiomac.2019.09.094.

Navaf, M., Sunooj, K. V., Aaliya, B., Sudheesh, C., George, J. 2020.Physico-Chemical, Functional, Morphological, Thermal Properties and Digestibility of Talipot Palm (Corypha Umbraculifera

*Correspondence: sulashisama@sjp.ac.lk

L.) Flour and Starch Grown in Malabar Region of South India. Journal of Food Measurement and Characterization. 14(3), 1601–1613. https://doi.org/10.1007/s11694-020-00408-1.

Nurazzi, N. M., Asyraf, M. R. M., Rayung, M., Norrrahim, M. N. F., Shazleen, S. S., Rani, M. S. A., Shafi, A. R., Aisyah, H. A., Radzi, M. H. M., Sabaruddin, F. A., Ilyas, R. A., Zainudin, E. S., Abdan, K.2021. Thermogravimetric Analysis Properties of Cellulosic Natural Fiber Polymer Composites: A Review on Influence of Chemical Treatments. Polymers (Basel). 13 (16). https://doi.org/10.3390/polym13162710.

Oh, S. Y., Yoo, D. Il, Shin, Y., Seo, G. 2005. FTIR Analysis of Cellulose Treated with Sodium Hydroxide and Carbon Dioxide. Carbohydrate Research. 340 (3), 417–428. https://doi.org/10.1016/j.carres.2004.11.027.

Petroudy, S. R. D. Physical and mechanical properties of natural fibers, in Fan M., Fu F.(Eds), Advanced High Strength Natural Fibre Composites in Construction, New York, pp. 59–84. https://doi.org/10.1016/B978-0-08-100411-1.00003-0

Porras, A., Maranon A., and Ashcroft I. A. 2015. Characterization of a Novel Natural Cellulose Fabric from Manicaria Saccifera Palm as Possible Reinforcement of Composite Materials. Composites Part B: Engineering. 74,66–73. doi: 10.1016/j.compositesb.2014.12.033.

Rajeshkumar, G., Devnani G. L., Prakash Maran J., Sanjay M. R., Suchart Siengchin, Naif Abdullah Al-Dhabi, and K. Ponmurugan. 2021. Characterization of Novel Natural Cellulosic Fibers from Purple Bauhinia for Potential Reinforcement in Polymer Composites. Cellulose. 28(9),5373–85. doi: 10.1007/s10570-021-03919-2.

Segal, L., Creely, J. J., Martin, A. E., Conrad, C. M.1959. An Empirical Method for Estimating the Degree of Crystallinity of Native Cellulose Using the X-Ray Diffractometer. Textile Research Journal. 29 (10), 786–794. https://doi.org/10.1177/004051755902901003.

Senthamaraikannan, P., and Kathiresan M. 2018. Characterization of Raw and Alkali Treated New Natural Cellulosic Fiber from Coccinia Grandis . L. Carbohydrate Polymers 186,332–43. doi: 10.1016/j.carbpol.2018.01.072.

Sreenivasan, V. S., Somasundaram, S., Ravindran, D., Manikandan, V., Narayanasamy, R. 2011. Microstructural, Physico-Chemical and Mechanical Characterisation of Sansevieria Cylindrica Fibres - An Exploratory Investigation. Materials & Design. 32 (1), 453–461. https://doi.org/10.1016/j.matdes.2010.06.004.

Vijay, R., Lenin Singaravelu D., Vinod A., Sanjay M. R., and Suchart Siengchin. 2019. Characterization of Alkali-Treated and Untreated Natural Fibers from the Stem of Parthenium Hysterophorus Characterization of Alkali-Treated and Untreated Natural Fibers. Journal of Natural Fibers.1–11. doi: 10.1080/15440478.2019.1612308.

Vijay, R., Lenin Singaravelu D., Vinod A., Sanjay M. R., Suchart Siengchin, and Mohammad Jawaid. 2019. Characterization of Raw and Alkali Treated New Natural Cellulosic Fibers from Tridax Procumbens. International Journal of Biological Macromolecules. 125,99–108. doi: 10.1016/j.ijbiomac.2018.12.056.

*Correspondence: sulashisama@sjp.ac.lk